Formation of Nanostructured Zeolite Particle Surfaces via a Halide/Grignard Route

Shu Shu, Shabbir Husain, and William J. Koros*

School of Chemical & Biomolecular Engineering, Georgia Institute of Technology, 311 Ferst Drive NW, Atlanta, Georgia 30332

Received April 8, 2007. Revised Manuscript Received June 6, 2007

A two-step reaction sequence, dealumination via thionyl chloride followed by reaction with a Grignard reagent, has created a nanoscale morphology that appears as significantly roughened outer surfaces on zeolite 4A particles. X-ray photoelectron spectroscopy (XPS) and X-ray diffraction (XRD) measurements revealed that such surface nanostructures are composed of $Mg(OH)_2$ crystals. The formation mechanism of this specific surface morphology was explored. It was discovered by solid-state ^{29}Si and ^{27}Al NMR and XPS surface analysis that thionyl chloride partially removes aluminum from the zeolite 4A framework and yields NaCl and $AlCl_3$. Precipitation of these extracted inorganic salts on the surfaces of zeolite particles occur. Subsequently, methylmagnesium bromide is reacted with 2-propanol in a quenching process and generates $Mg(OH)_2$. The previously deposited NaCl and $AlCl_3$ nanoparticles on zeolite surfaces are believed to function as heterogeneous nuclei for the growth of $Mg(OH)_2$ crystals and thereby creates the nanostructured surface morphology. The modified particles are shown in previous work to provide enhanced interfacial adhesion in polymeric composites.

Introduction

The incorporation of inorganic silicate materials into polymeric matrix has been explored extensively as an efficient way for improving various performances such as thermal stability,[1] optical properties,[2] electrical properties,[3] catalytic reactivity,[4] and transport properties of materials.[5,6] Nevertheless, because of limited intrinsic compatibility between inorganic materials and many organic polymers, lack of adhesion at the interfaces poses challenges for applications of such hybrid materials. Better control and tailoring of the nanoscale interfacial regions to optimize the desired properties would enable successful fabrication of composite materials.

In our recent work, we developed a new strategy to promote the interfacial adhesion in polymer/silicate composites by creating a nanoscale morphology, which appears as a significantly roughened outer surface on the fillers.[7,8] The dramatic increase in the topological roughness on the particle surfaces is believed to provide improved interaction at the interface via induced adsorption and physical interlocking of polymer chains on the particle surfaces.[7,9] Such a surface nanostructure was obtained by a two-step route: the particles were first treated with thionyl chloride, followed by exposure to methylmagnesium bromide (Grignard reagent). In this study, we explored the underlying chemical mechanism of how the above-mentioned halide/Grignard reagent route creates the demonstrated nanoscale surface morphology.

Similar chemical processes have been studied by other researchers on porous silica or silicate materials to attach alkyl moieties to the silicon surface. Bansal et al. developed a two-step procedure where the H-terminated Si surface was first chlorinated radically by PCl_5 and subsequently quenched with a Grignard reagent at 80 °C for 30 min to 8 days to form Si−C bonds.[10−12] Sunseri et al. studied complete methylation of silica surfaces using thionyl chloride as a chlorination reagent, along with subsequent methylation by methyllithium.[13] Clark et al. employed the use of CCl_4 to make chlorinated silica followed by reaction with a Grignard reagent.[14] Terry et al. used chlorine gas under ultraviolet excitation to replace H on the H−Si(111) surface, followed by immersion in alkyl lithium solution.[15] Vassylyev et al. reported surface modification of ZSM-5 type zeolites using a combined $SiCl_4$ and Grignard reagent route.[16] In addition, research has discovered that by direct exposure of porous silica to Grignard reagents, Si−C bonds could be created as well.[17] Nevertheless, to our knowledge, there has not been

* Author to whom correspondence should be addressed. Phone: 404.385.2845; fax: 404.385.2683; e-mail: wjk@chbe.gatech.edu.

(1) Zhang, J.; Hou, L. Y.; Xu, L.; Xu, Z. L. *Chem. Mater*. **1999**, *11*, 3177.
(2) Beecroft, L. L.; Ober, C. K. *Chem. Mater*. **1997**, *9*, 1302.
(3) Raghavan, S. R.; Riley, M. W.; Fedkiw, P. S.; Khan, S. A. *Chem. Mater*. **1998**, *10*, 244.
(4) Clark, J. H.; Macquarrie, D. J. *Chem. Commun.* **1998**, 853.
(5) Lu, X.; Manners, I.; Winnik, M. A. *Macromolecules* **2001**, *34*, 1917.
(6) Teshima, K.; Sugimura, H.; Takai, O. *Langmuir* **2003**, *19*, 8331.
(7) Shu, S.; Husain, S.; Koros, W. J. *J. Phys. Chem. C* **2007**, *111*, 652.
(8) Husain, S.; Koros, W. J. *J. Membr. Sci*. **2007**, *288*, 195.
(9) Douglas, J. F. *Macromolecules* **1989**, *22*, 3707.
(10) Bansal, A.; Li, X.; Lauermann, I.; Lewis, N. S.; Yi, S. I.; Weinberg, W. H. *J. Am. Chem. Soc*. **1996**, *118*, 7225.
(11) Bansal, A.; Lewis, N. S. *J. Phys. Chem. B* **2001**, *105*, 10266.
(12) Bansal, A.; Li, X.; Yi, S. I.; Weinberg, W. H.; Lewis, N. S. *J. Phys. Chem. B* **2001**, *105*, 10266.
(13) Sunseri, J. D.; Gedris, T. E.; Stiegman, A. E.; Dorsey, J. G. *Langmuir* **2003**, *19*, 8608.
(14) Clark, J. H.; Williamson, C. J. *J. Mater. Chem.* **1993**, *3*, 575.
(15) Terry, J.; Linford, M. R.; Wigren, C.; Cao, R.; Pianetta, P.; Chidsey, C. E. D. *J. Appl. Phys.* **1999**, *85*, 213.
(16) Vassylyev, O.; Hall, G. S.; Khinast, J. G. *J. Porous Mater*. **2006**, *13*, 5.

10.1021/cm070969n CCC: $37.00
Published on Web 07/17/2007

any report with regard to the use of halide/Grignard reagent reaction sequence on aluminum-containing zeolites to create specific surface morphologies on particles. In addition, our work presented here will demonstrate that with the presence of aluminum in the zeolite framework, the reaction will proceed via a different path from that of the discoveries by the above researchers.

Experimental Section

Surface Modification of Particles. Zeolite 4A, which is an aluminosilicate (Advanced Specialty Gas Equipment) with a characteristic 5 μm cubic form, was selected as the model dispersed phase. Samples of 5−7 g of 4A particles were placed in a three-neck reaction flask. All the particles and the glassware used in the treatment were first dried in a vacuum oven at 150 °C for 24 h, followed by flame-drying of the glassware with a propane torch prior to the treatment. Amounts of 80 mL of anhydrous toluene (99.8%, Aldrich) and 20 mL of thionyl chloride (99.5%, low ion solution, Aldrich) were added to the reaction flask which contained the 4A powders. Both liquids were transferred carefully through a dry transfer line to maintain a moisture-free environment. This dispersion was kept in a sonication bath (Model 1510, Branson) under room temperature for 12 h, after which toluene and extra thionyl chloride were evaporated by a constant nitrogen sweep through the system. Then 80 mL of anhydrous toluene and 15 mL of methylmagnesium bromide (3.0 M solution in diethyl ether, Aldrich) were added to the reaction flask in the same manner as described above. The dispersion was again kept in a sonication bath under room temperature for 12 h. After this, excess methylmagnesium bromide was quenched by anhydrous 2-propanol (99.5%, Aldrich), and the particles were collected through filtration and rinsed with 2-propanol followed by deionized water for several times.

Scanning Electron Microscopy. SEM images were obtained with SEM LEO 1530, equipped with a thermally assisted field emission gun operating at 10 keV.

NMR Measurements. ^{29}Si NMR spectra were recorded on a Bruker DSX-300 spectrometer equipped with a 7 mm MAS probe with resonance frequencies of 59.6 MHz. Magic angle spinning was carried out at a rotation speed of 5 kHz. Single $\pi/2$ radio frequency pulses (pulse length 5μs) were used with a repetition time of 10 s. ^{29}Si chemical shifts were referenced to 3-(trimethylsilyl)-1-propanesulfonic acid, sodium salt (0 ppm). ^{27}Al MAS spectra were obtained at 78.2 MHz by using the same spectrometer. The ^{27}Al chemical shifts were referenced to the external $Al(H_2O)_6^{3+}$ in saturated aqueous aluminum chloride solution. The measurements were performed with a spin rate of 6.5 kHz, 0.6 μs excitation pulse, and 0.2 s recycle delay.

X-ray Photoelectron Spectroscopy. XPS spectra were collected using a Surface Science model SSX-100 ESCA spectrometer equipped with an electron gun and a monochromator. The system used an Al Kα source ($h\nu$ = 1486.6 eV). Ejected photoelectrons were detected by a hemispherical analyzer that provided high sensitivity and resolution. The operating pressure in the analyzing chamber was below 5×10^{-9} Torr. For each sample, spectra were collected in such a way that the photoemission angle was varied from 70° to 20° at an interval of 5° (forward), and back from 20° to 70° at an interval of 5° (backward), and three more rounds of forward and backward.

X-ray Diffraction. X-ray diffraction data were collected with Ni-filtered Cu Kα radiation on a PanAlytical X'Pert PRO apparatus.

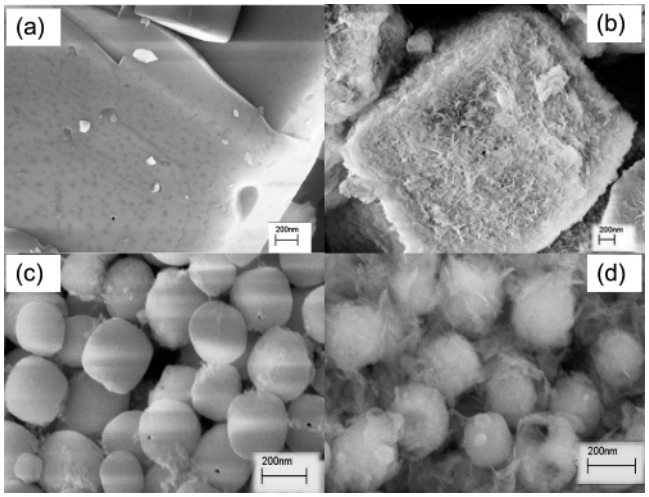

Figure 1. Representative scanning electron micrographs (SEM): (a) unmodified 5 μm 4A particle; (b) modified 5 μm 4A particle; (c) unmodified 200 nm 4A particles; (d) modified 200 nm 4A particles. Because of the difference in the sizes of the two types of sieves, the surface morphology appears as 'whiskers' on a large particle in micrograph b while it appears as 'cotton balls' on much smaller nanoparticles in micrograph d.

The samples were pressed into a sample holder with a microscope slide. Precautions were taken to avoid preferred orientation. The data were recorded by step-scanning at 0.02° 2θ per step from 5° to 60° 2θ, where θ is the Bragg angle, and a counting time of 1s for each step.

Results and Discussion

1. Characterization and Identification of Surface Nanostructure.

1.1. Characterization of Surface Morphology. Figure 1 displays the surface morphologies of zeolite 4A before and after the chemical treatment described earlier. Particles of two average diameters, 5 μm and 200 nm, were shown, respectively. These SEM images clearly show that a new nanoscale structure which appears as a significantly roughened surface has been created on the outer surfaces of the particles during this process. These modified particles, when incorporated into polymer matrixes, have greatly improved the interfacial adhesion between the polymer and sieve phases, as demonstrated by our previous work.[7,8] The roughened particle surface is believed to enhance the interfacial adhesion via thermodynamically induced adsorption and physical interlocking of polymer chains onto such random morphology. In order to identify which compound (or compounds) comprises such surface nanostructures, various characterization techniques were utilized.

1.2. XPS Elemental Characterization. X-ray photoelectron spectroscopy was conducted to reveal the changes in the surface elemental compositions of the particles and the results are shown in Figure 2. Figure 2a depicts the XPS survey of untreated zeolite 4A, where the major peaks correspond to the four elements of this material: Na, O, Si, and Al. After the two-step treatment, new peaks of Mg (~15% atomic concentration) were detected on the sieve surfaces as shown in Figure 2b. Evidently, the Mg-containing species is attributed to the new surface structure. Since there is negligible change in the carbon concentration on the surface as compared to the base value on the unmodified particles, these whiskers are very likely to be an inorganic

(17) Kim, N. Y.; Laibinis, P. E. *J. Am. Chem. Soc.* **1998**, *120*, 4516.

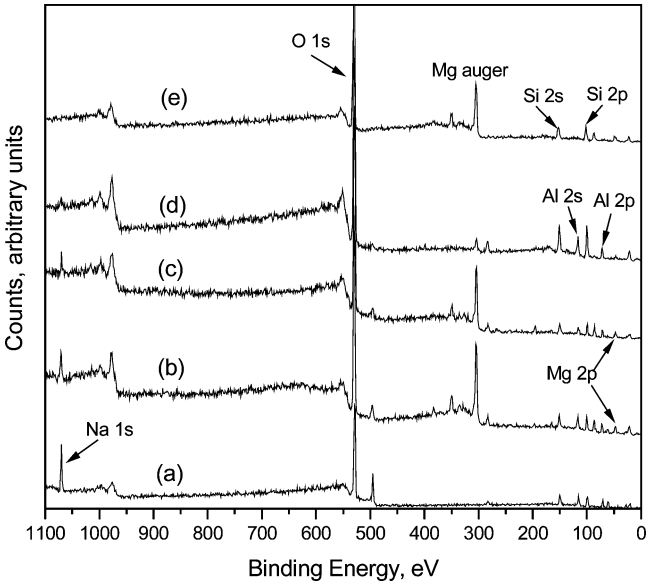

Figure 2. X-ray photoelectron survey spectra of zeolite 4A and pure silica particles after the surface treatment: (a) untreated zeolite 4A; (b) zeolite 4A treated by the halide/Grignard route; (c) same sample in (b) dried in air under 400 °C for 24 h; (d) same sample as in b, after exposure to dilute HCl solution; (e) pure silica particles treated using the same chemical process. The major peaks detected are Na 1s (1072 eV), O 1s (531 eV), Si 2s (151 eV), Si 2p (99 eV), Al 2s (118 eV), Al 2p (73 eV), Mg 2p (50 eV).

material. Two control steps were conducted to test this possibility. First, the treated 4A powders were dried in air at 400 °C for 24 h, followed by XPS analysis. Figure 2c illustrates the XPS spectrum for this sample, and negligible change was observed as compared to the sample before air drying (Figure 2b). This suggests that the Mg-containing compound is inorganic in nature; otherwise, air drying at 400 °C would have led to the degradation of common organic species. The second control test was to disperse the treated 4A sample in a dilute hydrochloride acid solution (0.1M) for 1 min. The sieves were then collected by centrifuge and rinsed repeatedly with deionized water. XPS spectrum for these HCl washed sieves is shown in Figure 2d. The intensities of Mg peaks for this sample diminished drastically, and only ~1.8% of Mg concentration was detected on the surface, as opposed to the original ~15% before the acid washing. This etching test further implies that it is highly possible that the surface magnesium-containing compound is an inorganic substance, such as magnesium oxide or magnesium hydroxide. Nevertheless, to further prove this hypothesis, the powder X-ray pattern was utilized to precisely identify this compound. In addition to zeolite 4A, pure silica particles were treated using the same halide/Grignard route. The reason for studying pure silica will be addressed later along with the XRD results. XPS survey for such treated silica also revealed the presence of Mg concentration on silica surfaces after the treatment, as can be seen in Figure 2e. Moreover, electron diffraction spectroscopy (EDS) was carried out to examine the bulk elemental concentrations of the modified 4A samples, and the results can be found in Supporting Information.

1.3. X-ray Diffraction. Powder X-ray diffraction was performed to further identify the Mg-containing compound on the particle surfaces. Initial attempts to measure the modified zeolite 4A particles did not yield any useful information. No difference was observed between the unmodified 4A and the modified counterparts. It may seem surprising at first but after careful consideration, it is not hard to explain the absence of diffraction peaks supposedly yielded by the surface nanostructure. Zeolite 4A is a very crystalline material; therefore, it generates a number of peaks with high intensities in an XRD test. These strong peaks of 4A tend to overwhelm the weak peaks produced by the Mg-containing species on the surface since the amount of such a nanostructure in the entire powder sample is very small as compared to the bulk 4A particles.

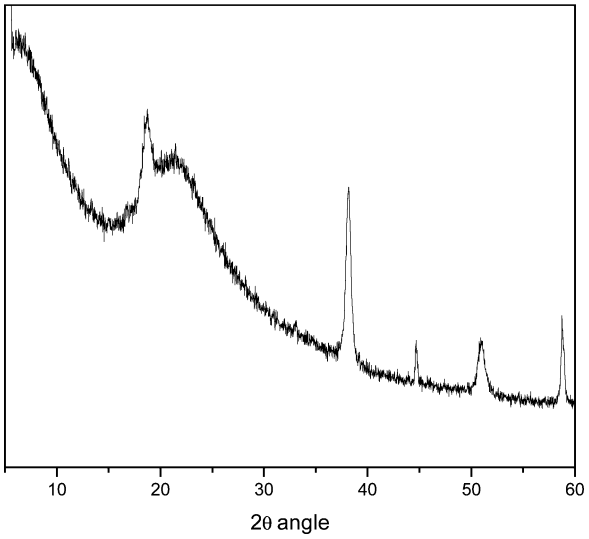

Figure 3. X-ray diffractogram of modified silica via the thionyl chloride/Grignard chemical treatment described in the present paper.

In order to avoid the interference caused by the fine crystallinity of zeolite 4A, pure silica was treated using the same procedure as described earlier. The great advantage of silica lies in the fact that it is an amorphous material; therefore, only an amorphous peak will show up in an XRD analysis without any additional diffraction signals. This will allow us to observe the diffraction peaks generated by the small amount of nanostructures on silica surface. XPS test exhibited the existence of Mg concentration on the treated silica particle surfaces as well (Figure 2e). The XRD diffractogram of such modified silica is shown in Figure 3. The broad peak from 15° to 30° is the amorphous region of silica. It is evident that the other peaks are produced by the surface magnesium compound. After careful indexing with the standard XRD powder patterns, it was found that these peaks correspond perfectly to magnesium hydroxide $Mg(OH)_2$. This finding explains the previous observations that the surface structure can resist air drying at 400 °C but is subject to HCl acid etching in an aqueous solution. Clearly $Mg(OH)_2$ could be dissolved by HCl to form water soluble $MgCl_2$, and thereby the surface structure was destroyed. In conclusion, work has identified that the surface nanostructure is composed of $Mg(OH)_2$ crystals.

2. Exploration of the Formation Mechanism of $Mg(OH)_2$ Nanostructure. The formation mechanism of the surface morphology is explored in this section. Since there are two reaction steps involved in the treatment, they are investigated individually to reveal the changes occurring in each step.

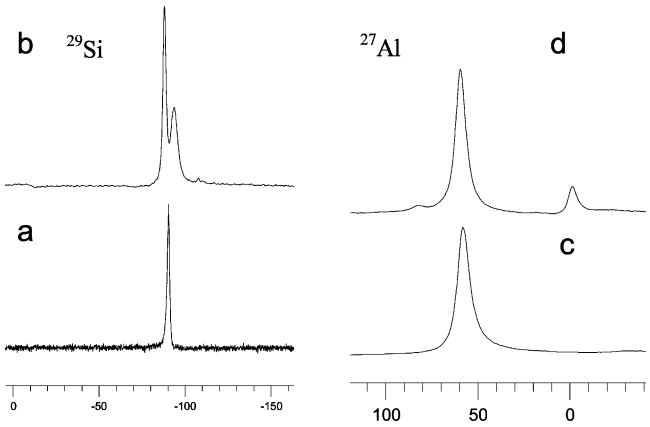

Figure 4. Solid-state NMR spectra: (a) ^{29}Si NMR spectrum of unmodified zeolite 4A; (b) ^{29}Si NMR spectrum of zeolite 4A after 12 h reaction with thionyl chloride; (c) ^{27}Al NMR spectrum of the same sample as in spectrum a; (d) ^{27}Al NMR spectrum of the same sample as in spectrum b.

2.1. Reaction Step One: Thionyl Chloride Treatment. In this section, zeolites were only treated with thionyl chloride. Solid-state ^{29}Si NMR and ^{27}Al NMR were utilized to reveal the possible structural changes after this reaction. Figure 4a and 4b illustrate the corresponding ^{29}Si MAS NMR spectra for the untreated and treated zeolite 4A. A single sharp peak at −90 ppm was detected for the unmodified sample, which is assigned to the inherent uniform Si (4Al) framework of zeolite 4A. In other words, each SiO_4^{4-} tetrahedron is surrounded by four AlO_4^{5-} tetrahedral units. After exposure to thionyl chloride for 12 h in a sonication bath, a new peak at −96 ppm showed up in the treated sample. This peak corresponds to the Si (3Al) blocks, which infers that some aluminum was removed from the framework of zeolite 4A after this reaction. ^{27}Al MAS NMR provided further evidence for such dealumination reaction. Figure 4c depicts the ^{27}Al NMR spectrum of the untreated 4A. A single, relatively narrow signal is seen with a chemical shift at 60 ppm corresponding to tetrahedrally coordinated aluminum in zeolite framework. Figure 4d shows the ^{27}Al NMR spectrum of the sample after reacting with thionyl chloride for 12 h. Unlike the fresh 4A sample, there are two peaks present: the one at 60 ppm corresponding to aluminum still remaining in tetrahedral sites and the other with a chemical shift of around 0 ppm corresponding precisely to Al in octahedral coordination. The latter peak is clearly generated by aluminum that has been removed from the zeolite framework. To summarize, these solid-state NMR spectra indicate that thionyl chloride has partially removed aluminum from 4A structure. This reaction has been reported in literature to occur at elevated temperatures, above 300 °C.[18] However, in our study it was induced by constant sonication under room temperature. More details regarding the effect of sonication on such dealumination reaction can be found in our recent work.[19]

XPS surface analysis was employed to examine the products of the dealumination reaction by thionyl chloride, and Figure 5 summarizes the results. Figure 5a demonstrates the surface survey of the fresh zeolite 4A sample, which

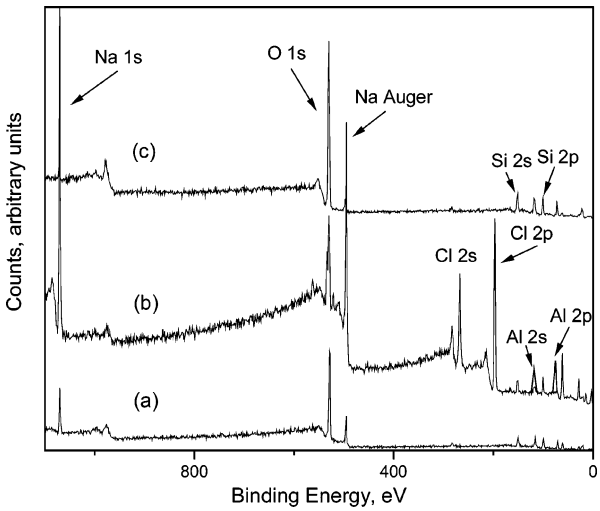

Figure 5. X-ray photoelectron spectra of 4A samples: (a) untreated zeolite 4A; (b) 4A after reaction with thionyl chloride; (c) sample b after rinse with deionized water. The major peaks detected are Na 1s (1072 eV), O 1s (531 eV), Si 2s (151 eV), Si 2p (99 eV), Al 2s (118 eV), Al 2p (73 eV), Cl 2s (271 eV), Cl 2p (200 eV).

consists of Na, O, Si, and Al. After the thionyl chloride treatment, substantial chlorine concentration was detected on the surfaces of the sieves (Figure 5b). Strong peaks at 271 eV (Cl 2s) and 200 eV (Cl 2p) appeared, indicating that this procedure yielded Cl-containing species on the sieve surfaces. The chlorine concentration is attributed to NaCl and $AlCl_3$, which are byproducts of the dealumination reaction.[18,19] A significant increase in the sodium concentration was observed at 1072 eV (Na 1s), which can be readily explained by the production of NaCl during the dealumination process. Our observation here is consistent with literature reports where researchers suggested the yield of NaCl after dealumination of sodium-containing zeolites,[20,21] which in our case is sodium-containing zeolite 4A. In addition to the increase in sodium concentration, the intensity of Al 2p peak is higher than that on the fresh 4A surface, which infers the enrichment of Al-containing substance on the treated zeolite surfaces. As shown earlier in Figure 4d, ^{27}Al NMR also detected nonframework aluminum species in this sample. These two results together imply the presence of $AlCl_3$ on the surfaces of the thionyl chloride-treated sieves, which agrees well with Fejes and co-workers' observations.[18]As a control step, the dealuminated 4A zeolites were washed repeatedly with deionized water, followed by XPS examination. It was found that the chlorine peaks disappeared after the rinsing step, and the intensity of Na 1s and Al 2p peaks also diminished significantly, which can be readily explained by the fact that NaCl and $AlCl_3$ were dissolved by water. The spectrum for this sample is shown in Figure 5c. Furthermore, the information regarding the proposed reaction mechanism of zeolite 4A by thionyl chloride can be found in our other publication.[19]

To summarize the first reaction, thionyl chloride acts as a dealumination reagent and partially removes aluminum from

(18) Fejes, P.; Kiricsi, I.; Hannus, I.; Kiss, A.; Schobel, G. React. *Kinet. Catal. Lett.* **1980**, *14*, 481.
(19) Shu, S.; Husain, S.; Koros, W. J. *Ind. Eng. Chem. Res.* **2007**, *46*, 767.
(20) Anderson, M. W.; Klinowski, J. *J. Chem. Soc., Faraday Trans.* **1986**, *82*, 1449.
(21) Klinowski, J.; Thomas. J. M.; Fyfe, C. A.; Gobbi, G. C.; Hartman, J. S. *Inorg. Chem.* **1983**, *22*, 63.

Scheme 1. Reaction Mechanism of Methylmagnesium Bromide with 2-Propanol

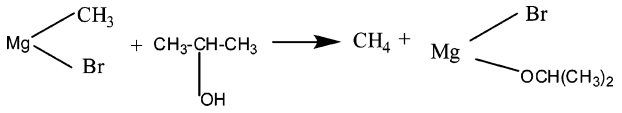

zeolite 4A framework. The two byproducts of this reaction, NaCl and $AlCl_3$, precipitate on the particle surfaces afterward. The significance of these two salts in the formation of the final nanomorphology will be discussed in the subsequent section.

2.2. Reaction Step Two: Grignard Reagent. Obviously the Grignard reagent used in this work (methylmagnesium bromide) provided the source of magnesium for the surface $Mg(OH)_2$, because it is the only magnesium-containing compound used throughout the treatment. But how such a nanostructure was formed needs to be explored. Work described in this section aims to reveal this underlying chemical mechanism.

2.2.1. How Magnesium Hydroxide Is Produced. The first attempt is to identify through which process $Mg(OH)_2$ crystals are produced. There is an important step in our experimental procedure which is to quench the Grignard reagent with 2-propanol. During this process, a large amount of gas was released, accompanied by the formation of a white precipitate. This Grignard reaction is described to proceed via the mechanism depicted in Scheme 1.[22,23]

The liberated gas observed in our quenching process is methane. However, the basic magnesium halide is only described as 'tends to separate from the liquid phase as a white precipitate' without defining what this precipitate actually consists of. However, this product is critical in our study because it is possible that such precipitate contains $Mg(OH)_2$, the compound that comprises the surface morphology.

To explore this possibility, small amount of methylmagnesium bromide solution was mixed with 2-propanol. An excess amount of 2-propanol was added in order to ensure no methylmagnesium bromide remained since it is a highly flammable and corrosive reagent. The white precipitate generated from this reaction was collected by centrifuge, followed by drying under vacuum for 24 h. Elemental analysis by XPS and X-ray powder diffraction were conducted to examine the composition of such white powder. Three elements were detected by XPS survey (Figure 6a): O, Mg, and Br, which could possibly comprise $MgBr_2$, $Mg(OH)_2$/MgO. The powder diffraction pattern, on the other hand, generated a series of strong peaks corresponding well to $MgBr_2$, as shown in Figure 7a. It was also noted that there were a few weak peaks at 2θ values of 38° and 51° which could not be assigned to $MgBr_2$. Nevertheless, the intensities of these peaks were too small to index this material precisely. In order to eliminate the peaks yielded by $MgBr_2$ in the XRD test, further control was done to reveal the other substance which generated the weak peaks at 2θ of 38° and 51°. The

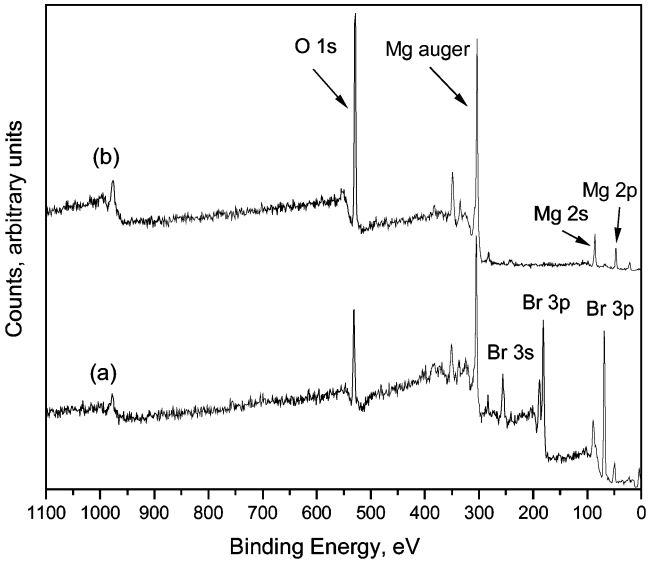

Figure 6. XPS analysis of the products from the reaction of methylmagnesium bromide with 2-propanol: (a) the white precipitates collected after the reaction; (b) the same sample, after being rinsed with deionized water, as in spectrum a. The major peaks detected are O 1s (531 eV), Br 3s (256 eV), Br 3p (182 eV), Br 3d (70 eV), Mg 2s (89 eV), Mg 2p (50 eV).

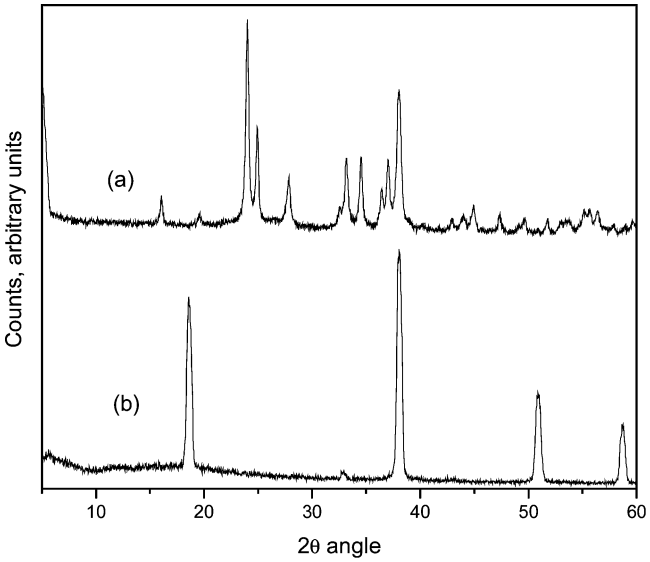

Figure 7. XRD diffraction patterns of: the products from the reaction of methylmagnesium bromide with 2-propanol: (a) the white precipitates collected after the reaction; (b) the same sample, after being rinsed with deionized water, as in spectrum a.

white precipitate collected from the Grignard/2-propanol reaction was dispersed in deionized water, in order to dissolve $MgBr_2$, as it is a water soluble salt. It was observed that although most of the white precipitate was dissolved immediately, there was small amount of white powder insoluble in water. This remaining powder was collected by centrifuge and rinsed with abundant deionized water, followed by drying. Again, XPS and XRD were performed to identify this powder sample, whose results are displayed in Figure 6b and 7b. It is clear that the Br peaks disappeared completely because all the $MgBr_2$ was dissolved by water. The insoluble powder is composed of Mg and O, whose XRD pattern corresponds perfectly to the $Mg(OH)_2$ diffraction pattern (Figure 7b). This experiment also explains why it was difficult to observe $Mg(OH)_2$ peaks in an XRD test for

(22) Fieser, L. F. Fieser, M. *Organic Chemistry*; Reinhold: New York, 1956.
(23) Bruice, P. Y. *Organic Chemistry*; Pearson Prentice Hall: Upper Saddle River, NJ, 2007.

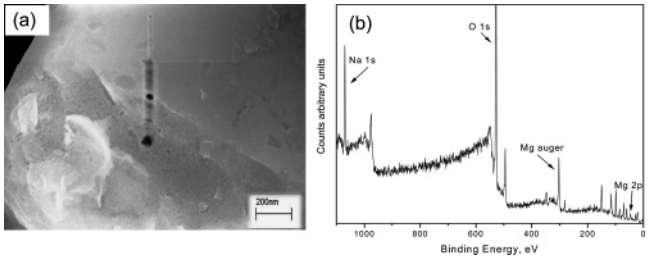

Figure 8. Sieve characterization results: (a) Representative SEM image of zeolite 4A particle treated only with methylmagnesium bromide/2-propanol; (b) XPS surface survey of sample a. The major peaks detected are Na 1s (1072 eV), O 1s (531 eV), Si 2s (151 eV), Si 2p (99 eV), Al 2s (118 eV), Al 2p (73 eV), Mg 2p (50 eV).

the bulk reaction precipitate. As was observed, the majority of such a precipitate is $MgBr_2$ which itself is a crystalline salt. Thus, the high-intensity peaks of $MgBr_2$ are likely to have overwhelmed the peaks yielded by the small amount of $Mg(OH)_2$. This phenomenon is similar to the previous zeolite 4A case, where the bulk 4A peaks covered the weak signals from the small amount of surface nanostructures.

The above investigations show that during the quenching process of methylmagnesium bromide with 2-propanol, $MgBr_2$ and $Mg(OH)_2$ are both produced and precipitated from the liquid phase. In our study, toluene was the liquid phase in which the solids were dispersed. The most likely scenario is that $MgBr_2$ and $Mg(OH)_2$ precipitated from toluene and encapsulated the zeolite particles. Later these zeolites were rinsed with deionized water in the experimental procedure and $MgBr_2$ was dissolved away from the particle surfaces. The finally collected particles after water rinsing only had $Mg(OH)_2$ remaining on the surface, which comprises the nanomorphology as shown in Figure 1.

2.2.2. How the Specific Surface Morphology Was Created. After determination of the chemical process that produced $Mg(OH)_2$, efforts were directed toward identifying how the specific surface morphology was formed. It was intuitive to assume that during the reaction of Grignard reagent with 2-propanol, this surface structure was created because this process yielded $Mg(OH)_2$, the component of such morphology. A control experiment was conducted to test this assumption, which was to expose zeolite 4A only to methylmagnesium bromide and 2-propanol without the preceding thionyl chloride step. SEM images were taken for these treated sieves, and XPS was used to analyze the surface elemental composition, the results of which are shown in Figure 8. As can be seen in Figure 8a, no apparent surface morphology was observed as compared to the significantly roughened surfaces of sieves treated with the two-step sequence (Figure 1). However, XPS still detected the presence of Mg concentration on these sieve surfaces (Figure 8b), which implies that Grignard/2-propanol reaction yielded $Mg(OH)_2$ but it did not have the specific crystalline morphology observed in Figure 1. The large 'chunks' in Figure 8a are likely to be some big $Mg(OH)_2$ crystals. These findings excluded the hypothesis that the Grignard reagent/2-propanol reaction itself created the roughened surface morphology. In other words, in order to form the specific surface pattern as shown in Figure 1, both reaction steps must be involved.

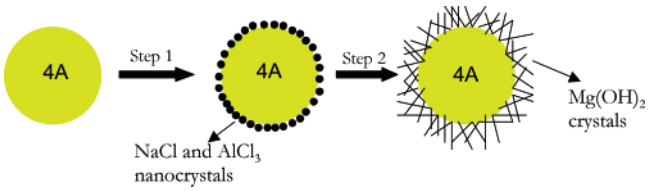

Figure 9. Illustration of the formation mechanism of the distinctive crystal morphology of $Mg(OH)_2$ on zeolite 4A surfaces.

As was discussed in 2.1 section, the direct result of the thionyl chloride reaction is that NaCl and $AlCl_3$ are generated and deposited on the surfaces of 4A particles. Without these salts, $Mg(OH)_2$ still precipitate on zeolite surfaces, but it does not have a defined crystal morphology. Therefore, it is hypothesized here that NaCl and $AlCl_3$ function as heterogeneous nuclei for the formation of $Mg(OH)_2$ fine crystals, thereby enabling $Mg(OH)_2$ to grow easily on the zeolite surface.[24] This process could have led to the specific 'whisker-like' crystal morphology. The proposed mechanism is illustrated in Figure 9. An experiment was performed to test this presumption. After the first reaction with thionyl chloride, zeolites were rinsed with abundant deionized water so that the NaCl and $AlCl_3$ were dissolved away. These rinsed particles were collected and dried, followed by exposure to methylmagnesium bromide and 2-propanol. No distinctive surface morphology was seen on such resultant particles. The SEM images were similar to Figure 8a. This observation provided further evidence that lack of surface nuclei (NaCl and $AlCl_3$) caused the absence of the distinctive morphology of $Mg(OH)_2$ on zeolite surfaces.

Another possibility is that the nanostructure formed on zeolite 4A belongs to MgAl species. This hypothesis was ruled out by a few facts. First, although the products of dealumination reaction are NaCl and $AlCl_3$, the concentration of Na is much higher than Al which can be observed in Figure 5b. Thus, the majority of the surface after dealumination was covered with NaCl and to a small extent $AlCl_3$. Furthermore, the most recent work by the authors involves directly depositing NaCl onto silica/silicate particle surfaces, followed by the Grignard reaction. Similar surface nanostructure was obtained, and XRD confirmed it is composed of $Mg(OH)_2$ crystals. This information will be included in our forth-coming publications. In principle, by intentionally depositing nuclei on the surfaces of particles, it is feasible to create similar nanostructures on the particle surfaces using the Grignard reaction. Current work in our group is exploring the above proposed mechanism and approach using surface seeding on materials other than zeolite 4A. It is expected that this chemical process could be extended to a broad array of inorganic materials.

3. Effect of These Modified Particles on Interfacial Adhesion. In our recent work, we have demonstrated the effect of such modified zeolites.[7,8] When incorporated into polymer matrixes, these particles provided greatly enhanced adhesion at the interfaces, thus forming defect-free polymeric composites with improved mechanical strength as well as gas separation efficiencies. The dramatic increase in the topological roughness (physical heterogeneity) on the sieve

(24) Mullin, J. W. *Crystallization*; Butterworth-Heinemann: Oxford, 2001.

surfaces is believed to provide stronger interaction at the interfaces via induced adsorption and physical interlocking of polymer chains in the nanoscopic surface structure.

Conclusion

A two-step reaction sequence, dealumination via thionyl chloride followed by reaction with a Grignard reagent, has created a nanoscale morphology that appears as significantly roughened outer surfaces on zeolite 4A particles. XPS and XRD measurements revealed that such surface nanostructures are composed of $Mg(OH)_2$ crystals. The formation mechanism of this specific surface morphology was explored. It was discovered by solid-state ^{29}Si and ^{27}Al NMR and XPS surface analysis that thionyl chloride partially removes aluminum from the zeolite 4A framework and yields NaCl and $AlCl_3$. Precipitation of these extracted inorganic salts on the surfaces of zeolite particles occur. Subsequently, methylmagnesium bromide is reacted with 2-propanol in a quenching process and generates $Mg(OH)_2$. The previously deposited NaCl and $AlCl_3$ nanoparticles on zeolite surfaces are believed to function as heterogeneous nuclei for the growth of $Mg(OH)_2$ crystals and creates the nanostructured surface morphology. The modified particles are shown in previous work to provide enhanced interfacial adhesion in polymeric composites.

Acknowledgment. The authors gratefully thank Medal L. P. for financial support of this work.

Supporting Information Available: EDS data of the modified zeolite 4A samples. This material is available free of charge via the Internet at http://pubs.acs.org.

CM070969N